Available online at www.CivileJournal.org

Civil Engineering Journal

(E-ISSN: 2476-3055; ISSN: 2676-6957)

Vol. 12, No. 06, June, 2026

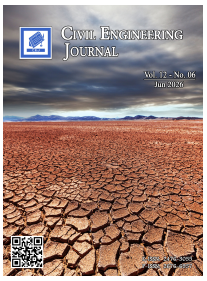

Vertical Design Response Spectra in Case of Varying Deep Geology and Moderate to High Seismicity

Borko Bulajić [1], Silva Lozančić [2], Dorin Radu [3*], Senka Bajić [4], Ercan Işık [5], Miljan Kovačević [6], Marijana Hadzima-Nyarko [2]

[1] *Faculty of Technical Sciences, University of Novi Sad, Trg Dositeja Obradovića 6, Novi Sad 21000, Serbia.*

[2] *Faculty of Civil Engineering and Architecture, Josip Juraj Strossmayer University of Osijek, Osijek 31000, Croatia.*

[3] *Faculty of Civil Engineering, Transilvania University of Braşov, Braşov 500152, Romania.*

[4] *Faculty of Applied Security, Educons University, Vojvode Putnika 85-87, Sremska Kamenica 21208, Serbia.*

[5] *Department of Civil Engineering, Bitlis Eren University, Bitlis 13100, Türkiye.*

[6] *Faculty of Technical Sciences, University of Pristina, Knjaza Milosa 7, Kosovska Mitrovica 38220, Serbia.*

Received 28 February 2026; Revised 15 May 2026; Accepted 23 May 2026; Published 01 June 2026

Abstract

This study aims to investigate the influence of local soil conditions and deep geological settings on vertical pseudo-spectral accelerations (*PSA*) and their relationship with horizontal *PSA* through vertical-to-horizontal (V/H) ratios, addressing limitations in current seismic design provisions. A case study is conducted for a representative site in Banja Luka, Bosnia and Herzegovina, characterized by moderate-to-high seismicity and varying deep geological conditions. Regional attenuation equations for the vertical response spectra are presented. Uniform Hazard Spectra (UHS) and V/H ratios are calculated and systematically compared with the recommendations of Eurocode 8 (the 2004 version) for Type 1 and Type 2 spectra. The findings reveal that both local soil and deeper geological structures significantly influence vertical response spectra, leading to substantial deviations in V/H ratios from those prescribed by Eurocode 8. These discrepancies suggest that current code provisions may underestimate vertical seismic demand in certain conditions, potentially affecting structural safety, resilience, and sustainable design. Although the results are derived from a case study in Banja Luka, they provide valuable insight for regions with similar seismic and geological characteristics, particularly where detailed deep geology data remain limited. When more vertical accelerograms become available and the database is enlarged, the presented attenuation equations may be updated, and the vertical UHS easily recalculated.

Keywords: Vertical Ground Motion; Uniform Hazard Spectra; Deep Geology Site Conditions; Local Soil; Regional Attenuation Equations; Vertical To Horizontal Spectral Ratios.

1. Introduction

Numerous researchers continue to study vertical ground motion response spectra. For instance, Hu et al. [1] have demonstrated that vertical spectra are strongly controlled by site, path, and source effects, and that non-ergodic models greatly increase prediction accuracy (reducing uncertainty by up to 44%). They also confirm that spatial variability in vertical motions is systematic rather than random, which supports the need for regional and site-specific models. Sharma

* Corresponding author: dorin.radu@unitbv.ro

https://doi.org/10.28991/CEJ-2026-012-06-03

et al. [2] acknowledge the need for physics-based simulations in vertical ground motion analysis and present an Artificial Neural Network (ANN)-based broadband model for vertical spectra. Additionally, in accordance with the results of current empirical research by Ramadan et al. [3], Smerzini et al. [4] introduce a period-dependent factor for the Vertical-to-Horizonal (V/H) response spectral ratios. Furthermore, instead of employing the V/H models, several researchers currently favor creating ground motion models solely for the vertical ground motion component [5, 6]. However, none of the mentioned studies takes into account the simultaneous effects of the deep geological site surrounding and local soil conditions on the vertical spectra.

This study's main objective is to ascertain how both local soil and deep geology affect the pseudo-absolute spectral acceleration (*PSA*) spectra for vertical ground motion direction, *PSAvert*. In this context, "local soil" pertains to a geotechnical definition of site conditions that takes into account only the soil layers over the first layer that has an average shear wave velocity (V_S) greater than 800 m/s. Usually, only the first 30 meters are considered, but in some cases, even the depth up to more than 100 meters is analyzed [7, 8]. Consequently, local soil conditions could be referred to as "shallow geology." On the other hand, geological settings that are hundreds of meters or several kilometers deep are referred to as "deep geology" [9] (see Table 1 and the schematic presentation shown in Figure 1).

Table 1. Definition of the categorical variables S_{L1}, S_{L1}, S_{G1}, and S_{G2}, which are used in Equation 1 to take into account the effects of the site conditions

Categorical Variables for Local Soil	Types of Local Soil	Categorical Variables for Deep Geology	Types of Deep Geology
$S_{L1} = 0$, $S_{L2} = 0$	"Rock" ($s_L = 0$)	$S_{G1} = 0$, $S_{G2} = 0$	Basement Rock ($s = 2$)
$S_{L1} = 1$, $S_{L2} = 0$	Stiff ($s_L = 1$)	$S_{G1} = 1$, $S_{G2} = 0$	Complex (intermediate) ($s = 1$)
$S_{L1} = 0$, $S_{L2} = 1$	Deep ($s_L = 2$)	$S_{G1} = 0$, $S_{G2} = 1$	Sediments ($s = 0$)

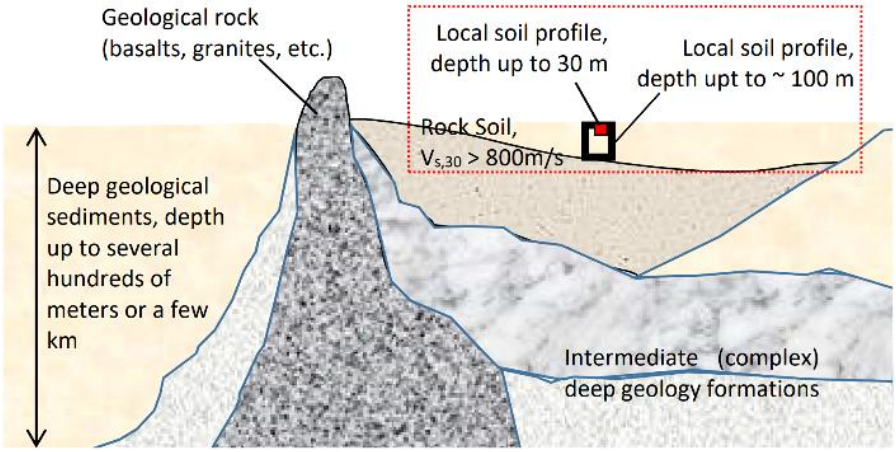

Figure 1. Schematic explanation of the difference between the "local soil" and "deep geology"

In this paper, for the local soil classification, we will refer to Seed et al. [7, 8]. Therefore, local soils having a layer thickness of less than 10 meters, above the layer with V_S > 800 m/s, will be referred to as "rock" soils (see Table 1). Sites with a 15–75 m deep soil layer on top of a V_S > 800 m/s layer will be referred to as "stiff soil." Lastly, soil layers thicker than 100 m above the V_S > 800 m/s layer will be referred to as "deep soil." Trifunac and Brady's classification system will be used for the deep geology [9]. Three categories of deep geology will be used: geological rocks (such as granites and basalts), deep geological sediments (which are typically found in large basins, such as the Pannonian basin), and intermediate locations with complex deep geological settings.

In this study, we continue to investigate strong ground motion prediction in areas with varying deep geology and with a history of moderate to strong destructive earthquakes. In our previous papers [10-12], we investigated the prediction of horizontal and vertical peak ground acceleration (PGA) and horizontal *PSA*. We have demonstrated that changes in deep geological conditions might affect horizontal PGA and *PSA* values more than local soil. When comparing the *PSA* amplitude at geological rock to that at intermediate sites, for example, the greatest site effects on the horizontal *PSA* are obtained at the vibration period of 0.1 s. In this instance, the site amplification (due to the deep geology) of 1.47 is 19% higher than the site amplification due to the local soil, which is equal to 1.24 for the stiff soil compared to the rock soil sites. The results of our vertical PGA analysis [11] show that the vertical to horizontal PGA ratios for the rock sites range from 0.30 to 0.66 and are dependent on the deep geology and source-to-site distance. Therefore, the single values of 0.90 and 0.45 that Eurocode 8 specifies for Type 1 and Type 2 spectra, respectively,

cannot be used to approximate these ratios. Furthermore, the findings of this study demonstrate that the effects of deep geology on vertical ground motion can also outweigh those of local soil [11]. Now, in this paper, our focus is on *PSAvert*.

For the case study location, we once again chose a site in Banja Luka, a city in Bosnia and Herzegovina. Banja Luka is located on the border between the Pannonian basin and the Dinaric Alps (see Figure 2) and has a diverse geological surroundings. The description of the regional seismotectonics and geological conditions underneath Banja Luka can be found in Geological guidebook through Bosnia and Herzegovina [13], a comprehensive study by Ustaszewski et al. [14], as well as in our accompanying papers [10-12] and will not be repeated here. On October 27, 1969, Banja Luka was devastated by the earthquake that had a magnitude of M_w=6.1. Its epicenter was only 10 kilometers from the Banja Luka city center, and in Banja Luka urban area, the observed intensity was VIII °MCS. Approximately 60% of buildings in Banja Luka were irreparably damaged [15, 16].

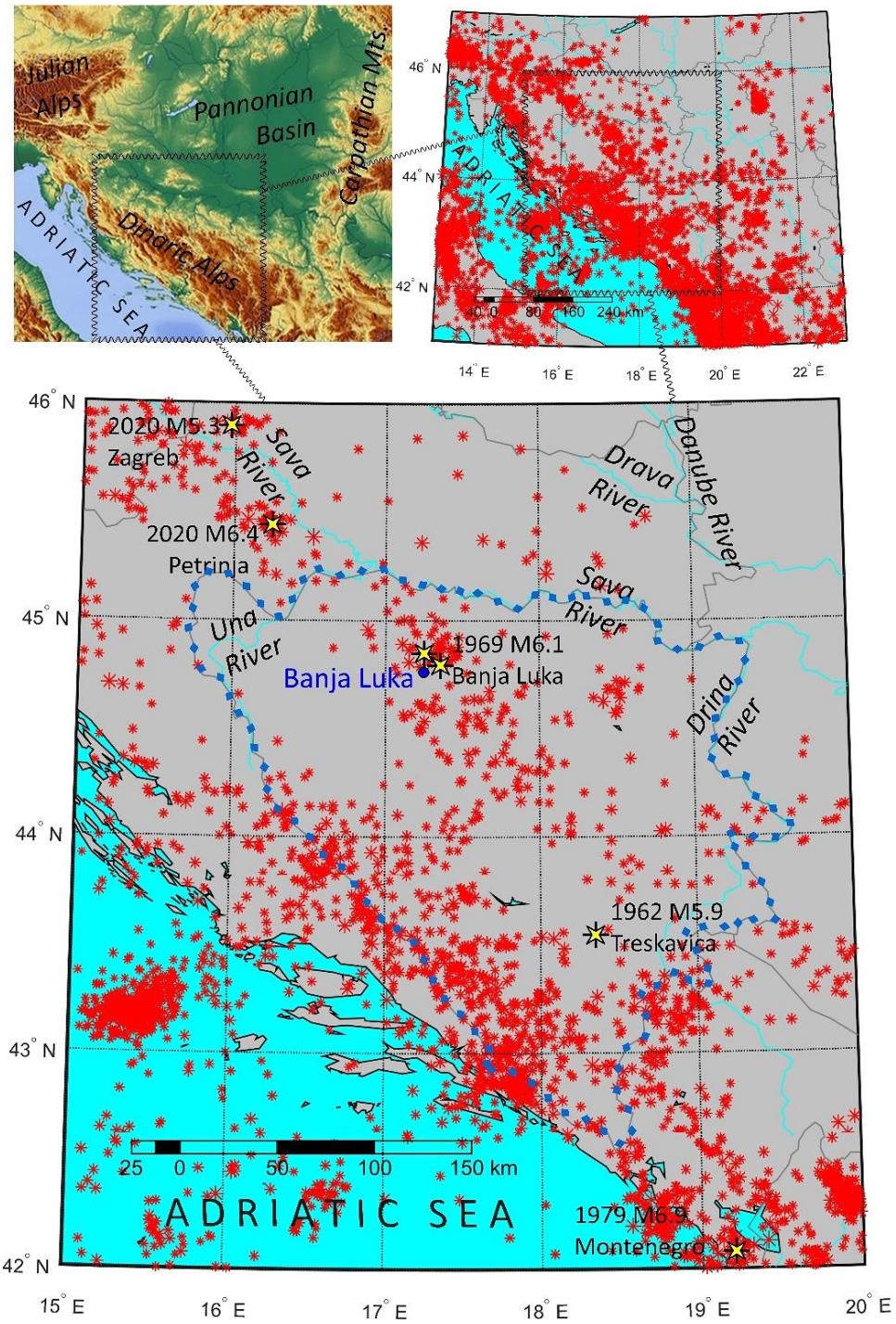

Figure 2. The top left shows the Dinaric and Julian Alps and Pannonian Basin; the top right shows the epicenters of the M_w≥3 earthquakes (1900 to 2025) [17]; and the bottom shows the location of Banja Luka (solid blue circle) and the most devastating seismic events in the region in contemporary history (1945–present).

In Eurocode 8 [18], which is used in Bosnia and Herzegovina [19], the vertical PGA is calculated by multiplying the official horizontal PGA value for the given location, which is specified for the "rock" (ground type A), by a constant that varies depending on the prevailing magnitudes. In the case of Eurocode 8 Type 1 spectra ($M > 5.5$), it is equal to 0.9, and in the case of Type 2 spectra ($M \leq 5.5$), it is 0.45. The motive for this particular study was the fact that Eurocode 8 [18], just like many other codes for earthquake-resistant design, neglects the effects of site conditions on the *PSAvert*. For both spectral types, vertical *PSA* spectra are identical for all ground types that are defined in Eurocode 8, implying that the site amplification occurs only horizontally, but not vertically. This complies with the H/V methodology for determining the natural period of vibration of local soil using microtremors, which was proposed by Nogoshi and Igarashi [20, 21] and subsequently made popular by Nakamura [22-24]. However, numerous investigations have shown that this approach does not always produce accurate results [25-29].

The vast majority of existing ground motion prediction equations (GMPEs) for PSA_{vert} only take local soil conditions into account by using the $V_{S,30}$ parameter [30-34]. Even though Eurocode 8 (Clause 3.1.2(1)) [18] allows for a different site classification that will account for the deep geology, neither Bosnia and Herzegovina nor any other country has not yet included the deep geological conditions in its National Annex [19, 35, 36]. However, PSA_{vert} estimates based on scaling equations that account for deep geology and local soil conditions for depths of up to 100 m or more have been shown to be quite accurate when compared to real strong motion records and observed intensities in the northwestern Balkans [37, 38]. Hence, we will first present empirical GMPEs for *PSAvert*, developed using only regional strong motion data. These scaling equations will consider both the effects of local soil conditions and deep geology. We also analyze vertical to horizontal spectral ratios, *VHpsa*, and compare them to the ones defined in Eurocode 8 [18] and by other researchers.

Finally, using the presented GMPEs, we will perform a probabilistic seismic hazard analyses (PSHA) and calculate the Uniform Hazard Spectra (UHS) for a location in Banja Luka, and compare the obtained UHS for PSA_{vert} to Eurocode 8 spectra. Furthermore, the vertical PGA multiplied by an assigned factor of 3.0 is how the peak spectral amplitudes are defined in Eurocode 8 [18]. Determining whether this spectral amplification factor produces precise maximum PSA_{vert} estimations is another objective of this study. It should be noted, however, that all of the analyses that are presented in this paper are based on seismicity, geology, and strong motion acceleration data that were collected solely in the northwestern Balkans. Therefore, in a strict sense, the findings should only apply to this region. However, until deep geology data for the vertical acceleration records are available in other regions, the results of this paper can be used as a preliminary case study for sites with similar seismicity and different deep geology situations.

Figure 3 provides a flowchart that succinctly illustrates how the proposed methodology results in the UHS that can be used as vertical design spectra in regions with moderate to high seismicity and varying deep geology conditions.

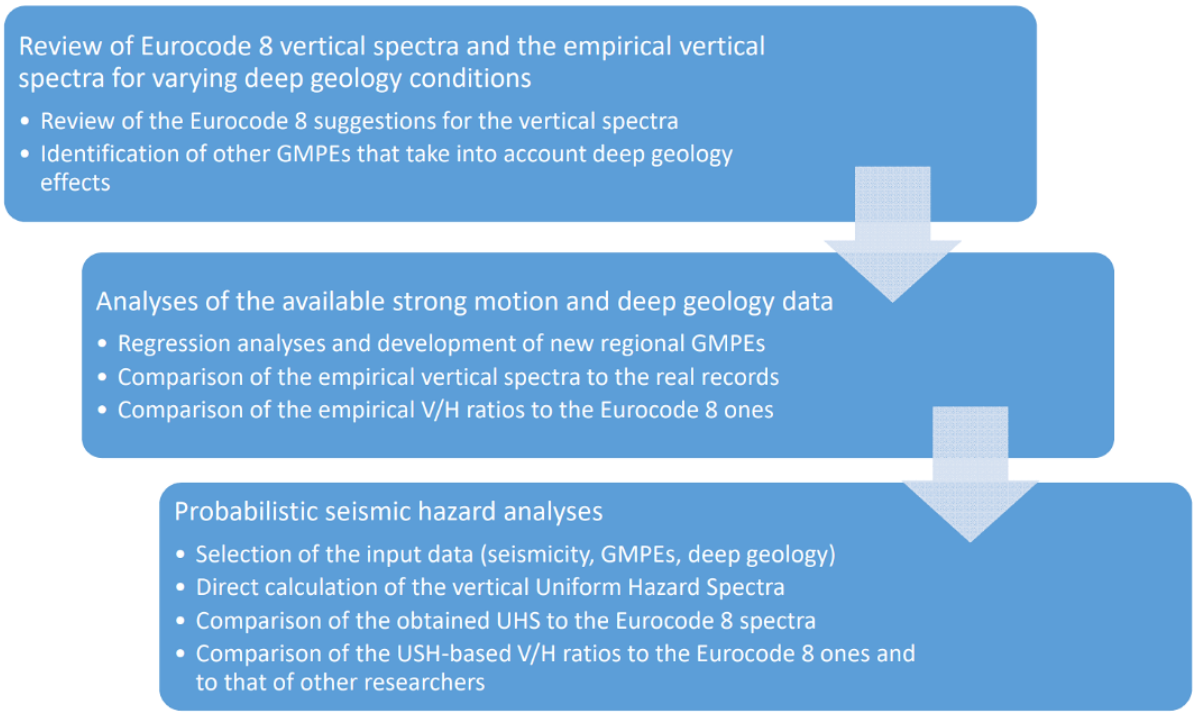

Figure 3. Flowchart of the proposed methodology that results in the vertical UHS that can be directly used as design spectra for the regions with varying deep geology and moderate to high seismicity

2. Empirical GMPEs for Vertical *PSA*

We begin by presenting empirical equations for calculating PSA_{vert} in regions with varying deep geological conditions. The GMPEs will be expressed using the mathematical form shown below.

$$\log[PSA_{vert}(T)] = a_1(T) + a_2(T) \cdot M + a_3(T) \cdot log(\sqrt{r^2 + r_0(T)^2}) + a_4(T) \cdot S_{L1} + a_5(T) \cdot S_{L2} + a_6(T) \cdot S_{G1} + a_7(T) \cdot S_{G2} + \sigma(T) \cdot P \quad (1)$$

where, T denotes the vibration period, M stands for earthquake magnitude, and r is the epicentral distance. Categorical variables S_{L1}, S_{L2}, S_{G1}, and S_{G2} are defined in Table 1. Scaling coefficients a_1 through a_6 result from the regression analysis – see Tables A1 and A2 in the Appendix I. We assumed that the data follow a log-normal distribution with a standard deviation $\sigma(T)$, and $P = 0$ for median estimations.

The database that was used for the regression analyses consists of 218 vertical components of strong motion acceleration time histories acquired in the northwestern Balkans from 112 different earthquakes with M ranging from 3 to 6.8 [11]. Further information regarding this database may be found in [10, 12, 39]. Even though the size of the available database of vertical ground motion records for various geological conditions in the northwestern Balkans is not large, this was the only region for which we had deep geology data for the acceleration records and the results of our analyses can be viewed as an initial step towards defining more reliable PSA_{vert} for both this and other regions with similar seismicity and geology. When more vertical accelerograms become available and the database is enlarged, the presented GMPEs for PSA_{vert} may be updated and the vertical UHS easily recalculated. Moreover, when deep geology data becomes available for the acceleration records in other regions, we will be able to compare the results and better assess robustness and transferability of our GMPEs.

The MATLAB® function "regress" was used to do multiple linear regression analysis. To lower the root mean squared error, r_0 (see Equation 1) was iteratively modified. We performed a secondary analysis utilizing only data from distances r of less than 30 km because more than half of the data was obtained across relatively short distances. In all analyses, we finally utilized the MATLAB® function "smooth" to smooth the coefficients a_1 to a_7 using weighted linear least squares and a second-degree polynomial model. Tables A1 and A2 show the final scaling coefficients, derived based on the strong motion data recorded at all distances and at distances of up to 30 km, respectively.

Figures 4 and 5 show the attenuation with epicentral distance of PSA_{vert} for six spectral amplitudes, that is, for T = 0.05, 0.10, 0.30, 0.50, 1.00, and 2.00 s. Figure 4 displays how the empirically obtained predictions of PSA_{vert} change with the deep geology, and Figure 5 shows how PSA_{vert} changes with the local soil types.

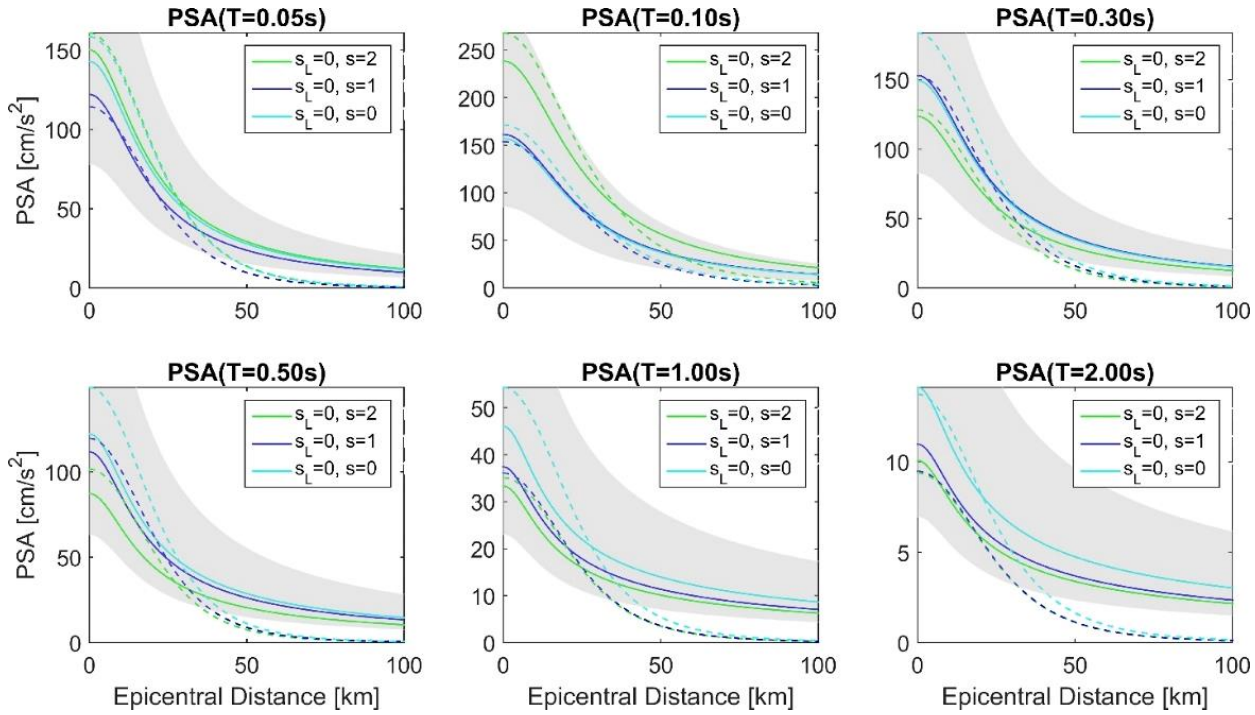

Figure 4. GMPEs for six different spectral amplitudes of PSA_{vert}, T = 0.05, 0.10, 0.30, 0.50, 1.00 and 2.00 s, calculated by Equation 1 and using Table A1 and Table A2 coefficients (solid lines and dashed lines, respectively), for s_L = 0 ("rock" type of local soil) and three different deep geology types, s (see Table 1). Gray area depicts the boundaries of the median ±σ estimates of PSA_{vert} for s=0.

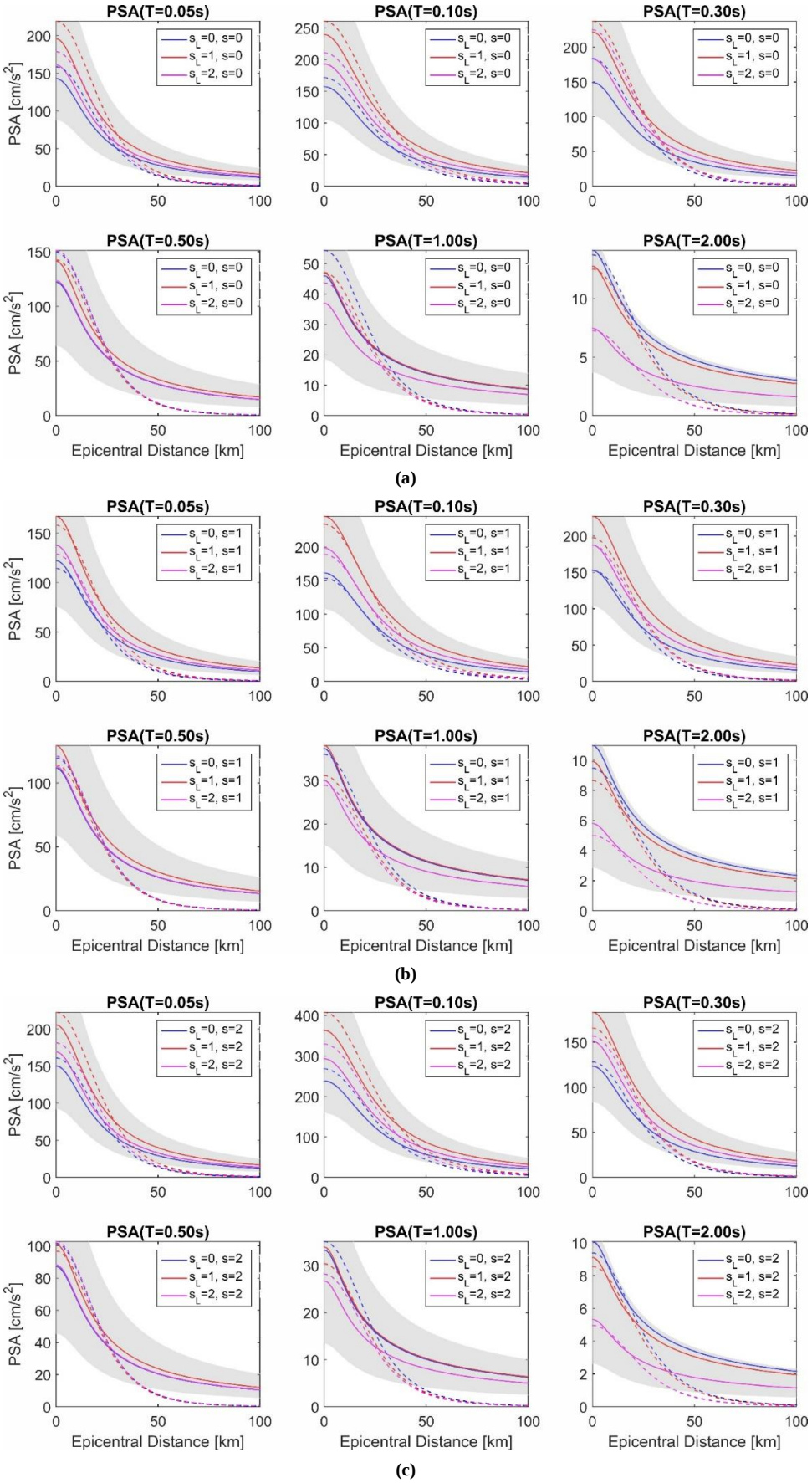

Figure 5. a) GMPEs for PSA_{vert} at six spectral amplitudes (T = 0.05, 0.10, 0.30, 0.50, 1.00 and 2.00 s), computed by Equation 1 and Table A1 and Table A2 coefficients (solid lines and dashed lines, respectively), for geological sediments (s = 0) and different types of local soil, s_L (see Table 1). The gray area shows the limits of the median ±σ estimates for s_L = 2, b) GMPEs for PSA_{vert}, for intermediate deep geological conditions (s =1) and different types of local soil, s_L, c) *GMPEs for PSA_{vert}, for deep geological rocks (s =2) and different types of local soil, s_L.*

To find the exact differences between the attenuation curves shown in Figures 4 and 5, we can use the scaling coefficients pertaining to categorical variables S_L and S_G. Table 2 shows the ratios between the empirical estimates of PSA_{vert} for different site conditions, calculated for 8 different spectral amplitudes using the scaling coefficients from Table A1.

Table 2. Ratios between the empirical $PSA_{vert}(T)$ estimates for different site conditions, calculated using the Table A1 coefficients, a_4 and a_5 for local soil, and a_6 and a_7 for deep geology

	Stiff / "Rock" soil (s_L = 1 / s_L = 0)	"Rock" / Stiff soil (s_L = 0 / s_L = 1)	Deep /"Rock" soil (s_L = 2 / s_L = 0)	"Rock" /Deep soil (s_L = 0 / s_L = 2)	Complex geology / Basement rock (s = 1 / s = 2)	Basement rock / Complex geology (s = 2 / s = 1)	Sediments / Basement rock (s = 0 / s = 2)	Basement rock / Sediments (s = 2 / s = 0)
T [s]	10^{a4}	$1/10^{a4}$	10^{a5}	$1/10^{a5}$	10^{a6}	$1/10^{a6}$	10^{a7}	$1/10^{a7}$
0.05	1.37	0.73	1.13	0.89	0.81	1.23	0.95	1.05
0.10	1.52	0.66	1.23	0.81	0.68	1.48	0.66	1.52
0.20	1.54	0.65	1.29	0.77	0.83	1.20	0.91	1.10
0.30	1.49	0.67	1.23	0.82	1.24	0.81	1.21	0.83
0.40	1.28	0.78	1.11	0.90	1.24	0.81	1.33	0.75
0.50	1.16	0.86	1.01	0.99	1.28	0.78	1.40	0.71
1.00	1.02	0.98	0.80	1.25	1.12	0.89	1.38	0.72
2.00	0.90	1.11	0.53	1.89	1.09	0.92	1.40	0.71

In case of deep geology, and if we use the coefficients from Table A1, $PSA_{vert}(T)$ for T = 0.05 s and T = 0.10 s will be $1/10^{-0.021}$ = 1.05 and $1/10^{-0.181}$ = 1.52 times larger at basement rocks (s = 2) than for the deep geological sediments (s = 0). This is possibly because high-frequency seismic waves travel through more compact geological formations more easily. However, the opposite is found for all vibration periods larger than 0.2 s; the PSA_{vert} for the geological rocks and T = 1.00 s is $1/10^{0.140}$ = 0.72 of the one obtained at deep geological sediments.

Regarding the effects of local soil, Table A1's coefficient a_5 shows positive values for all T up to 0.5 s. This suggests that for all vibration periods up to 0.5 s, the deep soil will cause an amplification of vertical ground motion. For instance, the PSA_{vert} in deep soil (s_L = 2) will be $1/10^{0.090}$ = 1.23 times greater than at rock sites (s_L = 0) for T = 0.10 s. However, the PSA_{vert} at T = 1.00 s will be de-amplified since $1/10^{-0.095}$ equals 0.80. This de-amplification may suggest that energy dissipation in deep soil surpasses the amplification because of the nonlinear behavior of soft sediments under strong ground motion. However, the fact that the de-amplification occurs only for vibration periods longer than 0.5 s was a surprising discovery because, according to Table A1 in Bulajić et al. [12], our analysis of the horizontal *PSA* spectra showed that de-amplification can be observed also for short-period waves. More precisely, in case of horizontal spectra, only the spectral amplitudes between T = 0.32 and T = 0.90 are amplified for the deep soil sites [12].

Table 2 shows that the effects of deep geology may be greater than those of local soil for some vibration periods. For instance, at the vibration period of 0.5 s, the maximum site amplification of 1.40 is achieved when comparing the PSA_{vert} for the geological sediments to that of the geological rock. The deep geology amplification is 21% higher than the local soil amplification of 1.16 for the same T at the stiff soil sites (relative to the "rock" soil).

The PSA_{vert} of 18 accelerograms recorded at four separate accelerograph stations in Banja Luka [11] is compared in Figure 6 with the empirical predictions calculated using Equation 1 and the scaling coefficients from Table A1. A high degree of agreement between the predicted and actual spectra is clearly seen.

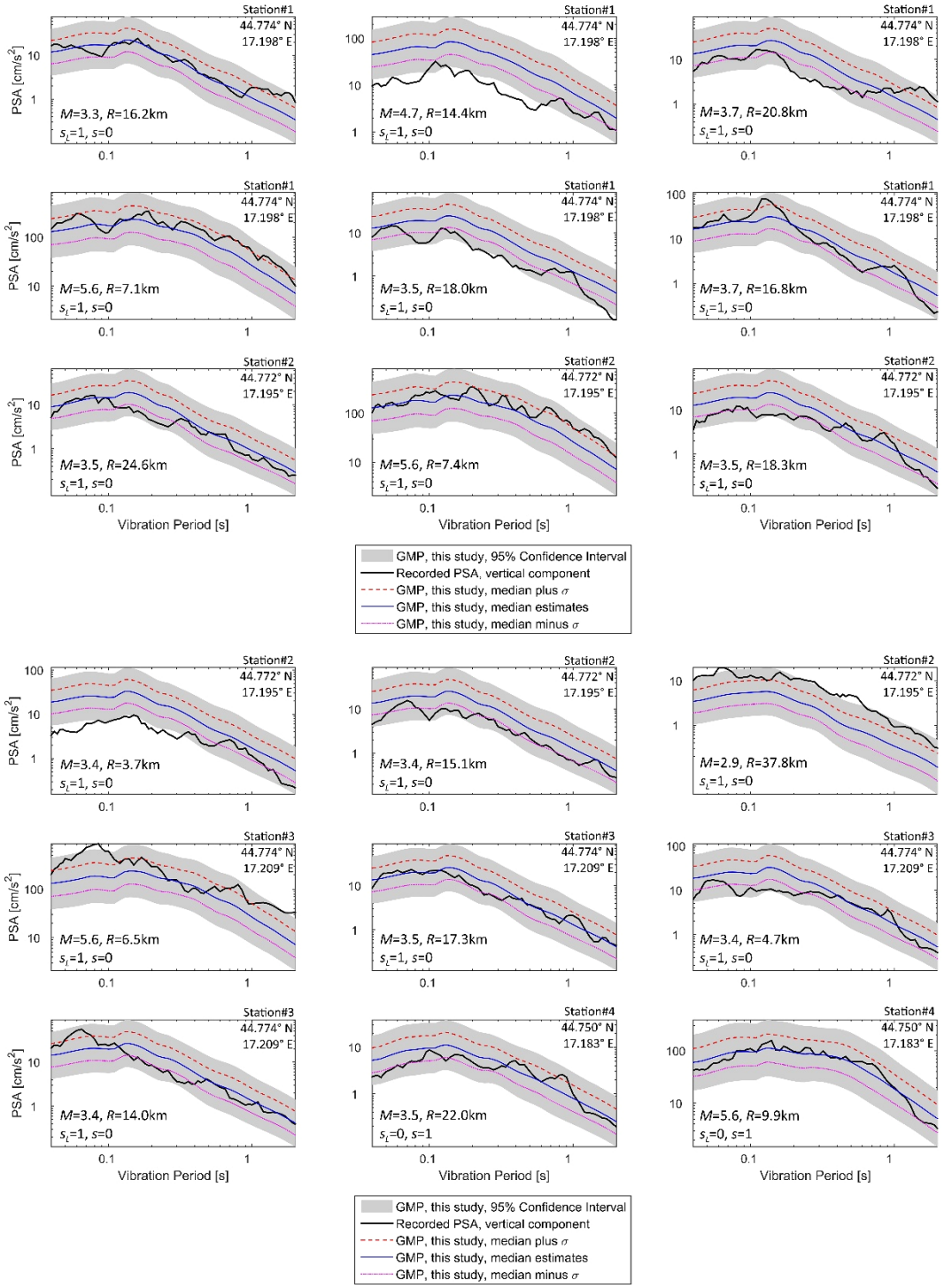

Figure 6. Recorded PSA_{vert} in Banja Luka in comparison to the empirical predictions that were derived from Equation 1 and Table A1 coefficients. The 95% confidence interval (corresponding to median ± 2·σ empirical estimates) is indicated by the gray area.

3. Ratios of Vertical *PSA* to Horizontal *PSA*

Figures 7 and 8 show how the ratios of vertical to horizontal empirical spectral estimates, *VHpsa*, change with epicentral distance and site conditions. The shown ratios were obtained by dividing the vertical *PSA*(*T*) calculated by Equation 1 and the Table A1 scaling coefficients (solid lines) and Table A2 (dashed lines) by the corresponding horizontal *PSA*(*T*) from Bulajić et al. [12]. The depicted ratios are also compared to the pertaining ratios that are suggested for Type 1 and Type 2 spectra in Eurocode 8 [18]. As can be seen, the distance to the earthquake source, vibration periods, local soil, and deep geology are all important and influence the *VHpsa*. As for the ratios suggested for Type 1 or Type 2 in Eurocode 8, these ratios differ dramatically from the empirically obtained ones. As can be observed from Figures 7 and 8, the empirical *VHpsa* is not a constant but rather changes in a non-linear manner with the distance. For longer periods, it has a tendency to become higher with *T*, while for shorter periods, the opposite trend occurs.

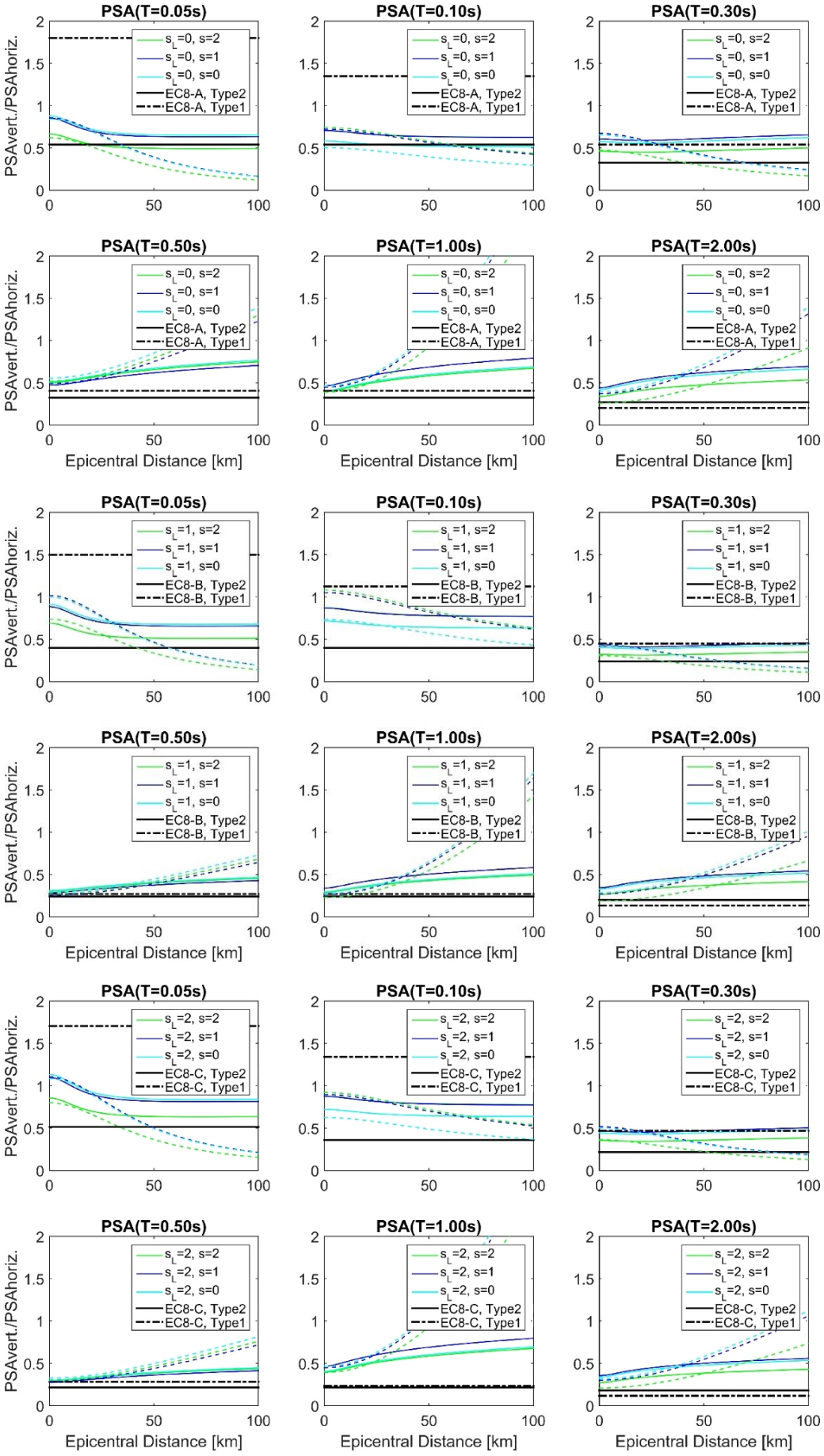

Figure 7. Empirical predictions of the *VHpsa* for six different spectral amplitudes (*T* = 0.05, 0.10, 0.30, 0.50, 1.00, and 2.00 s), obtained using Equation 1 and Table A1 and Table A2 coefficients (solid lines and dashed lines, respectively), for varying deep geological conditions (see Table 1).

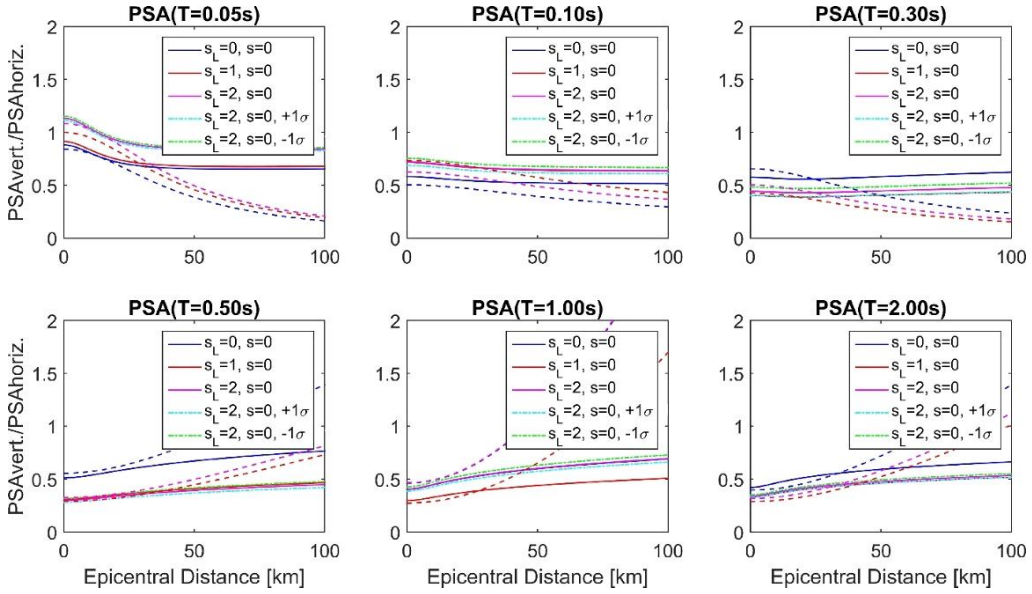

Figure 8. Empirical predictions of the *VHpsa* for six different spectral amplitudes (*T* = 0.05, 0.10, 0.30, 0.50, 1.00, and 2.00 s), obtained using Equation 1 and Table A1 and Table A2 coefficients (solid lines and dashed lines, respectively), for varying local soil conditions (see Table 1) and different probability levels of empirical estimates.

4. UHS Calculations for Vertical Ground Motion in Banja Luka

Next, we conduct a PSHA analysis for the case-study site with coordinates 44° 46.5' N, 17° 15' E, which are shown in Figure 9 as a solid blue circle. Equation 1 and the scaling coefficients from Table A1 are used in this study to define the GMPEs for PSHA analysis. The REASSESS V2.1 program [40] was used to compute the PSHA estimations. In the present study, we chose to employ the pan-European seismic source zone model, which represented one of the results of the SHARE ("Hazard in Europe") Project [41-43], even though the seismic source zones can be determined using accessible seismological data [44-46]. The new homogenous seismic catalogue that was created specifically for the SHARE project [47] serves as the basis for this source zone model. Details regarding the completeness, homogenization of magnitudes to M_W, and other critical factors of this catalogue are well examined in [42 ,48, 49] and will not be duplicated here.

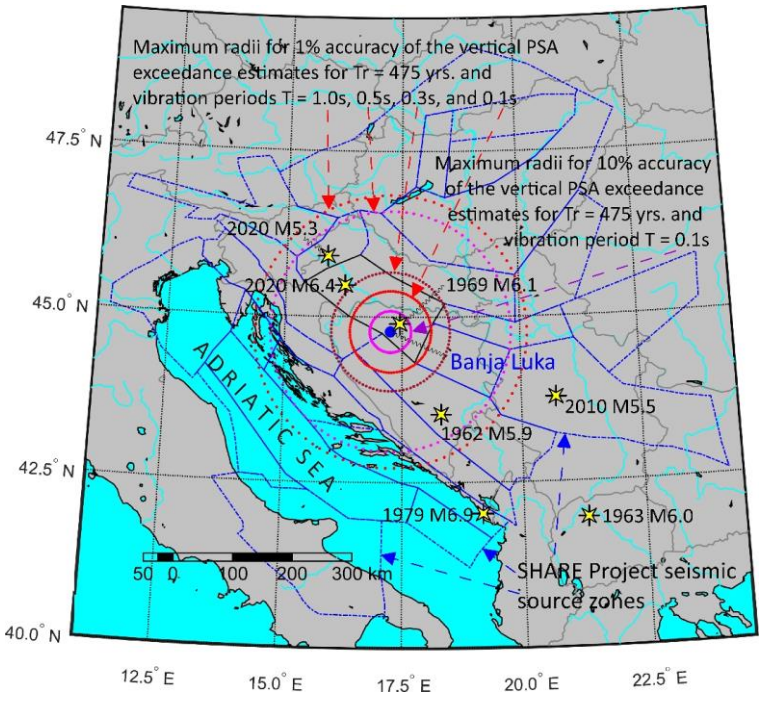

Figure 9. Map of the areal seismic source zones that were used in this study's PSHA analyses. The maximum radii for reaching 1 percent accuracy of the probabilitic estimates of *PSA*$_{vert}$ for vibration periods of 1.0, 0.5, 0.3, and 0.1 s are represented by the four larger circles around the analyzed location. The smallest circle represents the maximum radius for reaching 10 percent accuracy for the 0.1 s vibration period.

The epicentres of some of the strongest historical earthquakes and a few recent catastrophic earthquakes in the northwest Balkan region are depicted in Figure 9, along with the borders of the areal source zones used in this study's PSHA calculations. The source-to-site distances of 229 km, 202 km, 99.75 km, and 68.25 km are represented by the circles in Figure 9, and they are predicted to account for 99 percent of the total PSHA estimates for the 475-year return period for spectral amplitudes of 1.0, 0.5, 0.3, and 0.1 s, respectively. The smallest circle with a radius of 34.75 km represents the distances that will guarantee 10% accuracy of the 475-year PSHA calculations for the 0.1 s spectral amplitude. As anticipated, the circles illustrate that local seismicity will dominate short-period amplitudes, whereas distant strong earthquakes would have a larger effect on long-period PSA_{vert}.

In Figure 10, we present disaggregation of the hazard calculated for the location 44° 46.5' N, 17° 15' E, for three vibration periods (T) and two hazard probabilities. Probability of exceedance of 10% in 10 and 50 years corresponds to return period, Tr, of 95 and 475 years, respectively. Figure 11 displays a cumulative disaggregation for source-to-site distances and magnitudes, as well as the magnitude recurrence (Gutenberg-Richter) curve for the seismic zone around Banja Luka. Just as expected, the most contributing distances and magnitudes increase with the vibration period. The bottom-right plot in Figure 11 also shows real return periods for the magnitudes of 4.8, 5.15, 5.45, and 5.8. These magnitudes contribute to 50% of the seismic hazard for the PSA_{vert} at T = 0.1s and Tr = 95, 475, and 2475 years, and for the T = 1.0s and Tr = 475 years, respectively. Here, we should note that the so-called return period Tr is only a probabilistic measure that is equivalent to the reciprocal value of the mean annual rate of occurrence of seismic events that will cause a ground motion amplitude to exceed an expected value [10, 12]. Please refer to the relevant discussions in Bulajić et al. [10] and Bulajić et al. [12] for more information. Real return periods are much shorter than corresponding return periods, Tr, as seen in Figure 11. It's also crucial to keep in mind that, rather than using conservative limits for maximum magnitudes, Eurocode 8 [18] specifies spectral Types (1 or 2) in terms of the magnitudes that "contribute most to the seismic hazard defined for the site for the purpose of probabilistic hazard assessment." Based on what we see in Figures 10 and 11, it appears that for Banja Luka we ought to use the Type 2 spectra (defined in Eurocode 8 for magnitudes not exceeding 5.5).

As seen in Figures 10 and 11, only for longer T and longer Tr we may get the most contributing magnitude possibly larger than 5.5. Since the hazard maps that are part of a National Annex to Eurocode 8 are defined for PGA, the Type 2 spectra should be used for Banja Luka and regions with similar seismicity. However, the catastrophic 1969 Banja Luka Earthquake had a magnitude of 6.1, and this fact would lead multi-risk analysts to the conclusion that a risk associated with a 100-year return period flood, for examples, is to be combined with a seismic risk based on the 95-year official seismic hazard map for Bosnia and Herzegovina [19, 35-36], although we would rather need to use a 475-year map for that purpose.

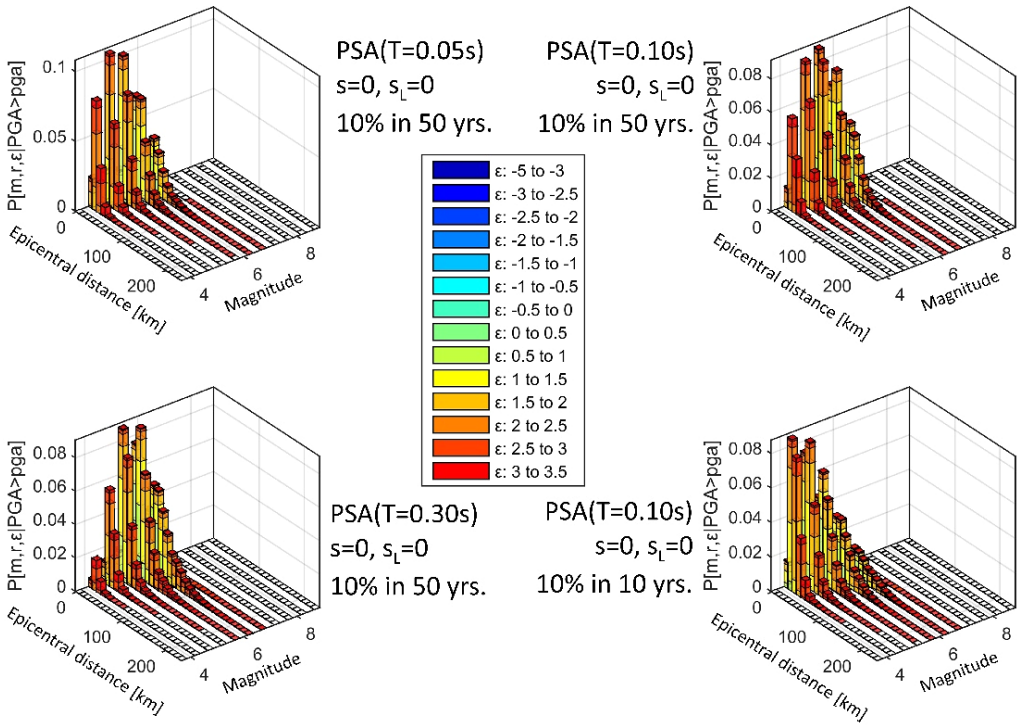

Figure 10. Disaggregation of calculated hazard for PSA_{vert} at the investigated location (44° 46.5' N, 17° 15' E), for different probabilities of exceedance and different spectral amplitudes

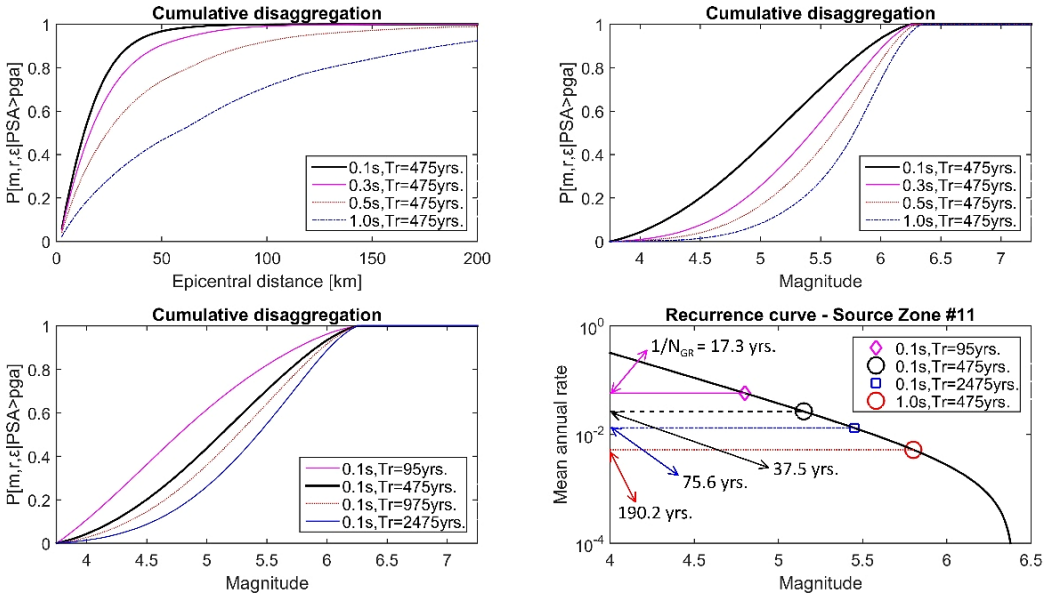

Figure 11. Cumulative disaggregation of seismic hazard for the analyzed site, calculated for distances (top-left plot) and magnitudes (top-right and bottom-left plots) and for different vibration periods and return periods. The magnitude recurrence curve for the seismic zone surrounding the analyzed site and entire city of Banja Luka (see Figure 9) is shown in the bottom-right plot.

Next, UHS spectra are calculated for the same site. In Figure 12, the left plots show the UHS calculated for the local soil defined as rock sites (s_L = 0), while the right plots show the UHS for stiff soil (s_L = 1). Top plots in Figure 12 compare the UHS with the Eurocode 8 Type 1 spectra, while bottom plots compare UHS to the Type 2 spectra. We can see that the vertical UHS amplitudes at the rock sites better fit the Type 2 Eurocode 8 spectra (bottom-left plot in Figure 12), while the UHS for the still soil better fit the Type 1 spectra (top-right plot). Table 3 displays the largest vertical UHS amplitudes for the probability of exceeding 10% in 50 years (Tr = 475 years), vibration periods (T) of these maximum UHS amplitudes, and the ratios S_{PGA} of the maximum vertical UHS amplitude to the vertical PGA. These ratios were computed for various site conditions. Table 3 demonstrates that for any analyzed combination of site conditions, we were unable to achieve the Eurocode 8 factor of 3.0. The S_{PGA} ratios are higher than the 3.0 ratio suggested by Eurocode 8 for all three types of local soil on top of deep geological rock, as well as for the deep soil sites on top of intermediate deep geology. For deep soils on top of geological rock we obtain the largest discrepancy, with S_{PGA} = 4.03, 34% higher than the ratio suggested by Eurocode 8. On the other hand, for all three types of local soil on top of deep geological sediments, as well as for the rock soil and stiff soil sites on top of intermediate deep geology, the S_{PGA} ratios are lower than the 3.0 ratio suggested by Eurocode 8. In these cases, the largest discrepancy is obtained for the rock soils sites on top of deep geological sediments, with the S_{PGA} ratio of 2.24, which is 25% lower than what is suggested by Eurocode 8.

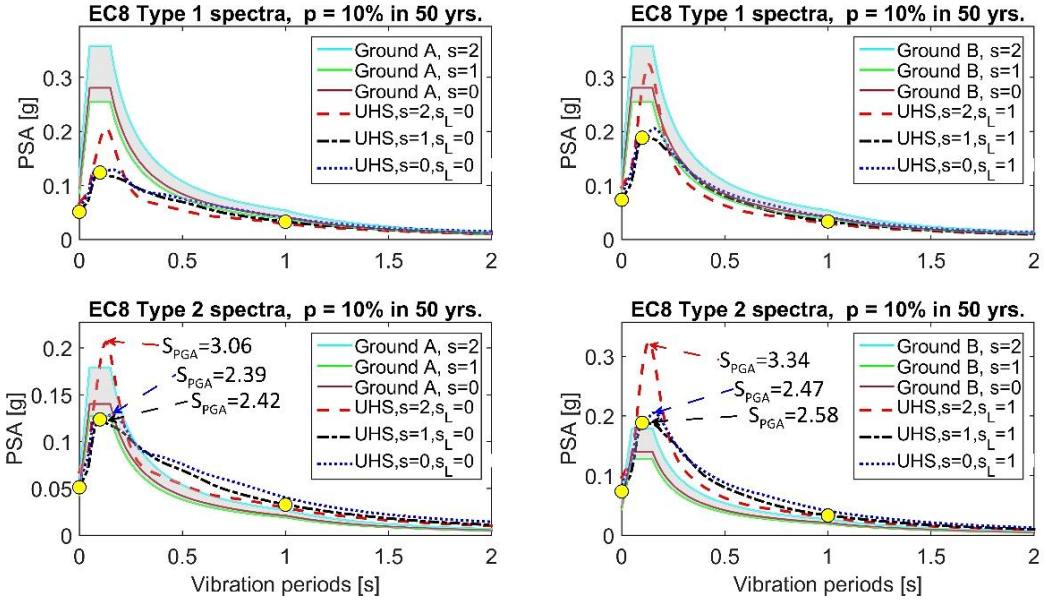

Figure 12. USH for vertical ground motion for different site conditions, compared to corresponding Eurocode 8 [18] Type 1 and 2 spectra (top and bottom plots, respectively), all calculated for the case-study site

Table 3. Maximum vertical 475-year UHS amplitudes and the corresponding vibration periods, as well as the ratios between the maximum vertical UHS amplitudes and vertical PGA values, S_{PGA}, calculated for different site conditions

	Deep geological rock (*s* = 2)			Intermediate deep geology sites (*s* = 1)			Deep geological sediments (*s* = 0)		
Local soil	**Maximum UHS [g]**	***T* [s]**	**S_{PGA}**	**Maximum UHS [g]**	***T* [s]**	**S_{PGA}**	**Maximum UHS [g]**	***T* [s]**	**S_{PGA}**
"Rock" (s_L = 0)	0.21	0.07	3.06	0.12	0.05	2.42	0.13	0.06	2.24
Stiff (s_L = 1)	0.32	0.10	3.34	0.19	0.07	2.58	0.21	0.08	2.47
Deep (s_L = 2)	0.26	0.07	4.03	0.15	0.05	3.11	0.17	0.06	2.99

As many codes try to simplify shapes of the design spectra and scale them by only one or two amplitudes, in Figure 12 we have also designated the vertical UHS amplitudes at 0.0s (vertical PGA), 0.1s, and 1.0s. Although it seems that these three UHS amplitudes may capture key points of the entire vertical spectra, we still see no reasons why the vertical design spectra should not be computed directly for at all spectral amplitudes for which scaling coefficients are available (in Tables A1 and A2, we presented scaling coefficients for 61 different vibration periods).

Finally, we estimate *VHpsa* for different combinations of site categorical variables (see Table 1), as shown in Figure 13. For different vibration periods, we compare the obtained *VHpsa* to the corresponding ratios suggested in Eurocode 8 [18] for Type 1 and Type 2 spectra. We also compare them to the only two GMPEs that we could find that used exactly the same categorical variables for the site conditions as we did (see Table 1). The first GMPEs are labeled USC-CA, and were created at the USC for California [50], whereas the ones labeled USC-ExYU were also created at the USC but for former Yugoslavia [51]. While both GMPEs neglect the local soil effects on vertical spectra, the equation for California, based on 1482 strong motion time histories, demonstrates that deep geology does influence seismic waves in the vertical direction [50].

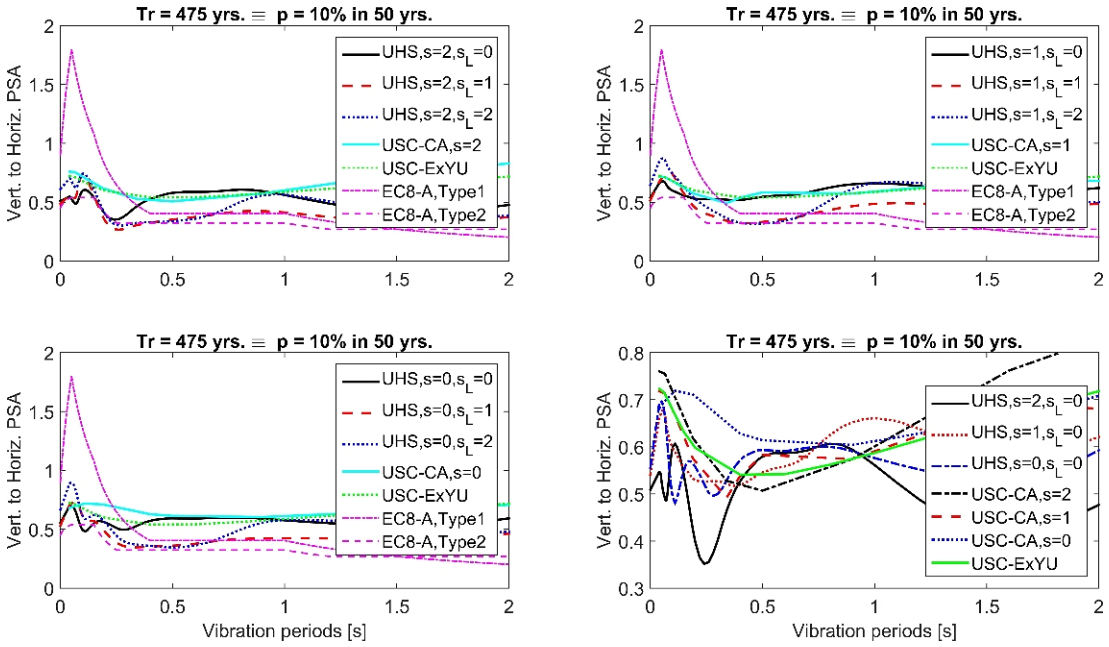

Figure 13. *VHpsa* for different site conditions, calculated by dividing vertical by horizontal UHS. Corresponding Eurocode 8 [6] ratios and the empirical estimates of *VHpsa* in California [23] (labeled USC-CA) and former Yugoslavia [24] (USC-ExYU) are also shown.

Figure 13 shows that the Eurocode 8 Type 2 *VHpsa* ratios are quite consistent with the *VHpsa* empirical predictions, however the Eurocode 8 *VHpsa* ratios computed for Type 1 spectra are substantially larger for shorter vibration periods. For the 0.05 s vibration period, the Eurocode 8 *VHpsa* ratio for Type 1 spectra is 1.8, which is two to three times more than other *VHpsa* ratios displayed in Figure 13. However, the *VHpsa* ratios obtained from the computed UHS amplitudes based on our GMPEs roughly match the *VHpsa* ratios produced by the empirical equations for California for intermediate (complex) deep geology (s = 1) and rock soil sites (sL = 0) for all vibration periods. For basement rock (s = 2) and deep sediments (s = 0), the *VHpsa* ratios derived from the UHS amplitudes agree with the ratios determined by the GMPEs for California. However, there is a discrepancy for vibration periods between 0.1 and 0.4, where "our" *VHpsa* ratios are 30–40% lower. Unfortunately, there are no additional GMPEs that simultaneously take into account the effects of local soil and deep geology, other from the GMPEs for California that are covered here [50]. As a result, they were the only ones to which our study's findings could be compared, notwithstanding that our GMPEs are based on 218 acceleration

components that were recorded in the northeastern Balkans, whereas the Californian GMPEs were based on the 1482 acceleration components recorded in California [50]. We intend to update the GMPEs for PSA_{vert} and compare the *VHpsa* ratios to the Californian ones once more as additional vertical accelerograms become available and the database is expanded. Then and only then will we be able to evaluate our GMPEs' resilience and transferability more accurately.

5. Conclusion

In this study we first developed regional empirical ground motion prediction equations (GMPEs) for vertical pseudo-spectral acceleration (*PSAvert*) based exclusively on regional strong-motion data recorded in the northwestern Balkans, and explicitly incorporating the combined effects of local soil conditions and deep geological structures. Using these models, vertical uniform hazard spectra (UHS) were derived and systematically compared with Eurocode 8 provisions, alongside an analysis of vertical-to-horizontal spectral ratios (*VHpsa*). The results clearly demonstrate that, contrary to current code assumptions, vertical response spectra are significantly influenced by site-specific conditions, with both shallow soil layers and deep geological features exerting comparable impacts on seismic demand. In some cases, changes in deep geological conditions might affect PSA_{vert} even more than local soil. For example, when comparing PSA_{vert} at deep sediments to that at geological rock, the amplification at the vibration periods of 0.5 s is 1.40, which is 21% higher than the maximum amplification due to the local soil, which is equal to 1.16 for the stiff soil compared to the rock soil sites. Furthermore, the findings indicate that vertical design spectra should not be defined as scaled versions of the vertical ones, but rather derived directly from period-dependent UHS based on regionally calibrated GMPEs.

Additional analyses reveal that the dominant earthquake scenarios contributing to seismic hazard vary with vibration period and return period, with larger magnitudes and greater source-to-site distances becoming more influential at longer periods. Importantly, the commonly used return period does not correspond to a specific design earthquake, highlighting its limitations as a physical descriptor of seismic input. The study also shows that *VHpsa* ratios cannot be represented by a constant value, as they depend on multiple interacting factors, including vibration period, distance, soil conditions, and deep geology. Similarly, the ratio between maximum vertical spectral acceleration and vertical PGA deviates from the constant factor proposed in Eurocode 8.

6. Declarations

6.1. Author Contributions

Conceptualization, B.B. and S.L.; methodology, B.B. and S.L.; formal analysis, B.B., S.L., D.R., and S.B.; investigation, B.B., D.R., E.I., M.K., and M.H.-N.; data curation, B.B.; writing—original draft preparation, B.B. and S.L.; writing—review and editing, B.B., S.L., D.R., S.B., E.I., M.K., and M.H.-N.; visualization, B.B. All authors have read and agreed to the published version of the manuscript.

6.2. Data Availability Statement

The data presented in this study are available in the article.

6.3. Funding and Acknowledgments

Some of the results presented in this scientific study were obtained through research activities within the scope of the project entitled HEIstorical - Strengthening Green and Digital Capacities in Higher Education Through Collaboration in Integrating Historical Buildings into a Sustainable and Digital Future (https://heistorical.unitbv.ro), jointly funded by the European Union under the Erasmus+ KA220-HED – Cooperation Partnerships in Higher Education program, project number 2025-1-RO01-KA220-HED-000364478.

For the first author, this research has been supported by the Ministry of Science, Technological Development and Innovation (Contract No. 451-03-34/2026-03/200156) and the Faculty of Technical Sciences, University of Novi Sad through project “Scientific and Artistic Research Work of Researchers in Teaching and Associate Positions at the Faculty of Technical Sciences, University of Novi Sad 2026” (No. 01-3609/1).

6.4. Conflicts of Interest

The authors declare no conflict of interest.

7. References

[1] Hu, L., Li, Y., Pan, W., Yang, H., & Ji, S. (2025). Nonergodic Ground-Motion Model for Vertical Response Spectra Using Offshore Ground Motions from Subduction Earthquakes near the Japan Trench Area. Bulletin of the Seismological Society of America, 115(5), 2464–2484. doi:10.1785/0120240280.

[2] Sharma, V., Author, H. K. A., Gade, M., & Dhanya, J. (2025). ANN-Based Ground Motion and Physics-Based Broadband Models for Vertical Spectra. Pure and Applied Geophysics, 182(2), 637–665. doi:10.1007/s00024-025-03660-y.

[3] Ramadan, F., Smerzini, C., Lanzano, G., & Pacor, F. (2021). An empirical model for the vertical-to-horizontal spectral ratios for Italy. Earthquake Engineering & Structural Dynamics, 50(15), 4121–4141. doi:10.1002/eqe.3548.

[4] Smerzini, C., Paolucci, R., Sgobba, S., & Ramadan, F. (2025). Vertical Seismic Action for Design: Developments for the Next Generation of European and Italian Norms. Earthquake Engineering & Structural Dynamics, 55(2), 350–362. doi:10.1002/eqe.70086.

[5] Phung, V. B., Abrahamson, N. A., Huang, B. S., & Loh, C. H. (2022). Vertical ground-motion prediction equation and the vertical-to-horizontal spectral ratio for crustal earthquakes in Taiwan. Earthquake Spectra, 38(2), 1189–1222. doi:10.1177/87552930211061168.

[6] Li, C., Ji, D., Zhai, C., Ma, Y., & Xie, L. (2023). Vertical ground motion model for the NGA-West2 database using deep learning method. Soil Dynamics and Earthquake Engineering, 165, 107713. doi:10.1016/j.soildyn.2022.107713.

[7] Seed, H. B., Muraka, R., Lysmer, J., & Idriss, I. M. (1976). Relationships of maximum acceleration, maximum velocity, distance from source, and local site conditions for moderately strong earthquakes. Bulletin of the Seismological Society of America, 66(4), 1323–1342. doi:10.1785/bssa0660041323.

[8] Seed, H. B., Ugas, C., & Lysmer, J. (1976). Site-dependent spectra for earthquake-resistant design. Bulletin of the Seismological Society of America, 66(1), 221–243. doi:10.1785/bssa0660010221.

[9] Trifunac, M. D., & Brady, A. G. (1975). On the correlation of seismic intensity scales with the peaks of recorded strong ground motion. Bulletin of the Seismological Society of America, 65(1), 139–162. doi:10.1785/bssa0650010139.

[10] Bulajić, B., Lozančić, S., Bajić, S., Starčev-Ćurčin, A., Šešlija, M., Kovačević, M., & Hadzima-Nyarko, M. (2025). Horizontal PGA Estimates for Varying Deep Geological Conditions—A Case Study of Banja Luka. Applied Sciences (Switzerland), 15(12), 6712. doi:10.3390/app15126712.

[11] Bulajić, B., Lozančić, S., Bajić, S., Starčev-Ćurčin, A., Šešlija, M., Kovačević, M., & Hadzima-Nyarko, M. (2025). PGA Estimates for Vertical Ground Motion and Varying Deep Geology Site Surroundings—A Case Study of Banja Luka. Applied Sciences (Switzerland), 15(12), 6542. doi:10.3390/app15126542.

[12] Bulajić, B., Lozančić, S., Bajić, S., Radu, D., Işık, E., Negovanović, M., & Hadzima-Nyarko, M. (2025). Horizontal UHS Predictions for Varying Deep Geology Conditions—A Case Study of the City of Banja Luka. Sustainability (Switzerland), 17(13), 6012. doi:10.3390/su17136012.

[13] Hrvatović, H. (2006). Geological guidebook through Bosnia and Herzegovina. Geological Survey of Federation Bosnia and Herzegovina, Sarajevo, Bosnia and Herzegovina.

[14] Ustaszewski, K., Herak, M., Tomljenović, B., Herak, D., & Matej, S. (2014). Neotectonics of the Dinarides-Pannonian Basin transition and possible earthquake sources in the Banja Luka epicentral area. Journal of Geodynamics, 82, 52–68. doi:10.1016/j.jog.2014.04.006.

[15] Trkulja, D. (2009). Earthquakes in Banja Luka. Proceedings of the International conference on earthquake engineering on the occasion of the 40 anniversary of Banja Luka Earthquake, 26-28 October, 2009, Banja Luka, Bosnia and Herzegovina.

[16] Trkulja, D. (2009). Earthquakes of Banja Luka Region. Institute of Construction Banja Luka – ZIBL, Banja Luka, Bosnia and Herzegovina.

[17] United States Geological Survey (USGS). (2025). Earthquake Catalogue for All Earthquakes with Mw ≥ 3.0 in the Period between 1900 and April 2025 for the Geographic Region between 41° N and 47° N, and 13° E and 23° E. United States Geological Survey (USGS), Reston, United States.

[18] EN 1998-1. (2004). Eurocode 8: Design of Structures for Earthquake Resistance. Part 1: General Rules, Seismic Actions and Rules for Buildings. European Committee For Standardization, Brussels, Belgium.

[19] BAS EN 1998-1/NA:2018. (2018). Seismic Zone Maps and Reference Ground Accelerations. Maps Accompanying National Annexes.

[20] Nogoshi, M., & Igarashi, T. (1970). On the Amplitude Characteristics of Microtremor (Part 1). Zisin (Journal of the Seismological Society of Japan. 2nd Ser.), 23(4), 281–303. doi:10.4294/zisin1948.23.4_281.

[21] Nogoshi, M., & Igarashi, T. (1971). On the Amplitude Characteristics of Microtremor (Part 2). Zisin (Journal of the Seismological Society of Japan. 2nd Ser.), 24(1), 26–40. doi:10.4294/zisin1948.24.1_26.

[22] Nakamura, Y. (2000). Clear identification of fundamental idea of Nakamura's technique and its applications. Proceedings of the 12th world conference on earthquake engineering, 30 January-4 February, 2000, Auckland, New Zealand.

[23] Nakamura, Y. (1989). A method for dynamic characteristics estimation of subsurface using microtremor on the ground surface. Railway Technical Research Institute, Quarterly Reports, 30(1), Railway Technical Research Institute/Tetsudo Gijutsu Kenkyujo, Tokyo, Japan.

[24] Nakamura, Y. (1996). Real-time information systems for seismic hazards mitigation: UrEDAS, HERAS and PIC. Quarterly Report of RTRI, 37(3), 112–127.

[25] Bonnefoy-Claudet, S., Köhler, A., Cornou, C., Wathelet, M., & Bard, P. Y. (2008). Effects of love waves on microtremor H/V ratio. Bulletin of the Seismological Society of America, 98(1), 288–300. doi:10.1785/0120070063.

[26] Rong, M., Fu, L. Y., & Li, X. (2017). On the amplitude discrepancy of HVSR and site amplification from strong-motion observations. Bulletin of the Seismological Society of America, 107(6), 2873–2884. doi:10.1785/0120170118.

[27] Imposa, S., Lombardo, G., Panzera, F., & Grassi, S. (2018). Ambient vibrations measurements and 1D site response modelling as a tool for soil and building properties investigation. Geosciences (Switzerland), 8(3), 87. doi:10.3390/geosciences8030087.

[28] Mucciarelli, M. (1998). Reliability and applicability of nakamura's technique using microtremors: An experimental approach. Journal of Earthquake Engineering, 2(4), 625–638. doi:10.1080/13632469809350337.

[29] Del Gaudio, V., Wasowski, J., & Muscillo, S. (2013). New developments in ambient noise analysis to characterise the seismic response of landslide-prone slopes. Natural Hazards and Earth System Sciences, 13(8), 2075–2087. doi:10.5194/nhess-13-2075-2013.

[30] Gülerce, Z., Kamai, R., Abrahamson, N. A., & Silva, W. J. (2017). Ground motion prediction equations for the vertical ground motion component based on the NGA-W2 database. Earthquake Spectra, 33(2), 499–528. doi:10.1193/121814EQS213M.

[31] Kalkan, E., & Gülkan, P. (2004). Empirical attenuation equations for vertical ground motion in Turkey. Earthquake Spectra, 20(3), 853–882. doi:10.1193/1.1774183.

[32] Bozorgnia, Y., & Campbell, K. W. (2016). Vertical ground motion model for PGA, PGV, and linear response spectra using the NGA-West2 database. Earthquake Spectra, 32(2), 979–1004. doi:10.1193/072814EQS121M.

[33] Kamai, R., Abrahamson, N. A., & Silva, W. J. (2016). VS30 in the NGA GMPEs: Regional differences and suggested practice. Earthquake Spectra, 32(4), 2083–2108. doi:10.1193/072615EQS121M.

[34] Campbell, K. W. (1997). Empirical near-source attenuation relationships for horizontal and vertical components of peak ground acceleration, peak ground velocity, and pseudo-absolute acceleration response spectra. Seismological Research Letters, 68(1), 154–179. doi:10.1785/gssrl.68.1.154.

[35] Ademović, N., Demir, V., Cvijić-Amulić, S., Málek, J., Prachař, I., & Vackář, J. (2021). Compilation of the seismic hazard maps in Bosnia and Herzegovina. Soil Dynamics and Earthquake Engineering, 141, 106500. doi:10.1016/j.soildyn.2020.106500.

[36] Ademović, N., Demir, V., Cvijić-Amulić, S., Málek, J., Prachař, I., & Vackář, J. (2023). Corrigendum to "Compilation of the seismic hazard maps in Bosnia and Herzegovina" [Soil Dynam. Earthq. Eng. 141 (2021) 106500]. Soil Dynamics and Earthquake Engineering, 164, 107633. doi:10.1016/j.soildyn.2022.107633.

[37] Bulajić, B., Hadzima-Nyarko, M., & Pavić, G. (2021). Vertical to horizontal UHS ratios for low to medium seismicity regions with deep soil atop deep geological sediments-an example of the city of osijek, Croatia. Applied Sciences (Switzerland), 11(15), 6782. doi:10.3390/app11156782.

[38] Bulajić, B., Pavić, G., & Hadzima-Nyarko, M. (2022). PGA vertical estimates for deep soils and deep geological sediments – A case study of Osijek (Croatia). Computers and Geosciences, 158, 104985. doi:10.1016/j.cageo.2021.104985.

[39] Jordanovski, L. R., Lee, V. W., Manic, M. I., Olumceva, T., Sinadinovski, C., Todoroska, M. I., & Trifunac, M. D. (1987). Strong earthquake ground motion data in eqinfos: yugoslavia part 1. Department of Civil Engineering, University of Southern California, Los Angeles, United States.

[40] Chioccarelli, E., Cito, P., Iervolino, I., & Giorgio, M. (2019). REASSESS V2.0: software for single- and multi-site probabilistic seismic hazard analysis. Bulletin of Earthquake Engineering, 17(4), 1769–1793. doi:10.1007/s10518-018-00531-x.

[41] Wiemer, S., Danciu, L., Edwards, B., Marti, M., Fäh, D., Hiemer, S., Wössner, J., Cauzzi, C., Kästli, P., & Kremer, K. (2015). European seismic hazard map for peak ground acceleration, 10% exceedance probabilities in 50 years. Swiss Seismological Service, Zürich, Switzerland. doi:10.2777/30345.

[42] Woessner, J., Laurentiu, D., Giardini, D., Crowley, H., Cotton, F., Grünthal, G., Valensise, G., Arvidsson, R., Basili, R., Demircioglu, M. B., Hiemer, S., Meletti, C., Musson, R. W., Rovida, A. N., Sesetyan, K., Stucchi, M., Anastasiadis, A., Akkar, S., Engin Bal, I., … Zschau, J. (2015). The 2013 European Seismic Hazard Model: key components and results. Bulletin of Earthquake Engineering, 13(12), 3553–3596. doi:10.1007/s10518-015-9795-1.

[43] Pagani, M., Garcia-Pelaez, J., Gee, R., Johnson, K., Poggi, V., Styron, R., ... & Monelli, D. (2018). Global Earthquake Model (GEM) Seismic Hazard Map (Version 2018.1–December 2018). GEM Foundation, Pavia, Italy.

[44] Amaro-Mellado, J. L., Melgar-García, L., Rubio-Escudero, C., & Gutiérrez-Avilés, D. (2021). Generating a seismogenic source zone model for the Pyrenees: A GIS-assisted triclustering approach. Computers & Geosciences, 150, 104736. doi:10.1016/j.cageo.2021.104736.

[45] Amaro-Mellado, J. L., Morales-Esteban, A., Asencio-Cortés, G., & Martínez-Álvarez, F. (2017). Comparing seismic parameters for different source zone models in the Iberian Peninsula. Tectonophysics, 717, 449–472. doi:10.1016/j.tecto.2017.08.032.

[46] Amaro-Mellado, J. L., & Bui, D. T. (2020). Gis-based mapping of seismic parameters for the pyrenees. ISPRS International Journal of Geo-Information, 9(7), 452. doi:10.3390/ijgi9070452.

[47] Stucchi, M., Rovida, A., Gomez Capera, A. A., Alexandre, P., Camelbeeck, T., Demircioglu, M. B., Gasperini, P., Kouskouna, V., Musson, R. M. W., Radulian, M., Sesetyan, K., Vilanova, S., Baumont, D., Bungum, H., Fäh, D., Lenhardt, W., Makropoulos, K., Martinez Solares, J. M., Scotti, O., … Giardini, D. (2013). The SHARE European Earthquake Catalogue (SHEEC) 1000-1899. Journal of Seismology, 17(2), 523–544. doi:10.1007/s10950-012-9335-2.

[48] Grünthal, G., & Wahlström, R. (2012). The European-Mediterranean earthquake catalogue (EMEC) for the last millennium. Journal of Seismology, 16(3), 535–570. doi:10.1007/s10950-012-9302-y.

[49] Grünthal, G., Wahlström, R., & Stromeyer, D. (2013). The SHARE European Earthquake Catalogue (SHEEC) for the time period 1900-2006 and its comparison to the European-Mediterranean Earthquake Catalogue (EMEC). Journal of Seismology, 17(4), 1339–1344. doi:10.1007/s10950-013-9379-y.

[50] Lee, V. W. (1987). Influence of Local Soil and Geologic Site Conditions on Pseudo Relative Velocity Spectrum Amplitudes of Recorded Strong Motion Accelerations. Issue CE 87-06, Department of Civil Engineering, University of Southern California, Los Angeles, United States.

[51] Lee, V. W., & Manic, M. (1994). Empirical scaling of response spectra in former Yugoslavia. Proceedings of the 10th European Conference on Earthquake Engineering, 28 August-2 September, Vienna, Austria.

Appendix I: Derived Scaling Coefficients for Vertical *PSA*

Table A1. Derived scaling coefficients of the empirical GMPEs, for the region of former Yugoslavia—Equation 1, based on the regional PSA_{vert} data that were recorded at all epicentral distances

T	a_1	a_2	a_3	r_0	a_4	a_5	a_6	a_7	σ
0.040	-1.545	0.370	-1.292	14.7	0.149	0.041	-0.091	-0.020	0.260
0.042	-1.524	0.369	-1.297	14.7	0.149	0.043	-0.090	-0.020	0.260
0.044	-1.502	0.369	-1.303	14.8	0.148	0.045	-0.090	-0.020	0.261
0.046	-1.476	0.368	-1.310	14.9	0.147	0.048	-0.090	-0.021	0.262
0.048	-1.436	0.366	-1.317	15.1	0.141	0.050	-0.090	-0.022	0.263
0.050	-1.399	0.364	-1.326	15.2	0.136	0.052	-0.090	-0.021	0.264
0.055	-1.307	0.362	-1.350	15.7	0.127	0.057	-0.090	-0.024	0.266
0.060	-1.222	0.361	-1.376	16.2	0.123	0.061	-0.092	-0.029	0.268
0.065	-1.145	0.362	-1.405	16.8	0.123	0.066	-0.094	-0.035	0.270
0.070	-1.082	0.365	-1.438	17.3	0.130	0.070	-0.097	-0.042	0.271
0.075	-1.006	0.371	-1.484	18.4	0.143	0.074	-0.104	-0.055	0.272
0.080	-0.937	0.376	-1.520	19.3	0.156	0.077	-0.113	-0.077	0.272
0.085	-0.875	0.378	-1.543	20.2	0.166	0.081	-0.125	-0.104	0.270
0.090	-0.824	0.378	-1.555	20.9	0.174	0.084	-0.140	-0.132	0.269
0.095	-0.791	0.378	-1.557	21.4	0.179	0.087	-0.155	-0.159	0.268
0.100	-0.774	0.377	-1.551	21.6	0.183	0.090	-0.170	-0.181	0.267
0.110	-0.776	0.376	-1.526	21.5	0.187	0.095	-0.199	-0.213	0.265
0.120	-0.809	0.375	-1.497	21.0	0.191	0.099	-0.224	-0.225	0.267
0.130	-0.862	0.378	-1.476	20.4	0.196	0.102	-0.237	-0.220	0.268
0.140	-0.914	0.386	-1.477	20.2	0.200	0.105	-0.234	-0.202	0.270
0.150	-0.974	0.396	-1.486	20.2	0.201	0.107	-0.219	-0.178	0.271
0.160	-1.042	0.408	-1.500	20.3	0.201	0.109	-0.195	-0.151	0.272
0.170	-1.122	0.420	-1.510	20.4	0.199	0.110	-0.168	-0.121	0.273
0.180	-1.213	0.431	-1.511	20.4	0.196	0.111	-0.139	-0.093	0.274
0.190	-1.310	0.440	-1.504	20.2	0.192	0.111	-0.109	-0.066	0.273
0.200	-1.408	0.449	-1.493	19.9	0.188	0.111	-0.080	-0.041	0.272
0.220	-1.596	0.460	-1.456	19.4	0.183	0.109	-0.027	0.002	0.269
0.240	-1.764	0.466	-1.407	18.8	0.184	0.106	0.020	0.035	0.265
0.260	-1.919	0.469	-1.354	18.2	0.185	0.101	0.056	0.057	0.261
0.280	-2.064	0.475	-1.310	17.5	0.181	0.095	0.079	0.071	0.259
0.300	-2.214	0.482	-1.265	16.7	0.172	0.088	0.093	0.083	0.259
0.320	-2.368	0.492	-1.222	15.7	0.161	0.081	0.099	0.091	0.262
0.340	-2.526	0.503	-1.181	14.7	0.148	0.072	0.098	0.100	0.266
0.360	-2.671	0.515	-1.147	13.7	0.134	0.064	0.095	0.108	0.270
0.380	-2.796	0.525	-1.118	13.0	0.121	0.055	0.093	0.115	0.273
0.400	-2.902	0.533	-1.093	12.5	0.109	0.046	0.094	0.123	0.277
0.420	-2.992	0.539	-1.072	12.2	0.098	0.037	0.095	0.129	0.279
0.440	-3.061	0.543	-1.053	12.2	0.088	0.029	0.099	0.134	0.282
0.460	-3.122	0.546	-1.036	12.1	0.079	0.021	0.102	0.139	0.284
0.480	-3.175	0.548	-1.019	12.1	0.070	0.013	0.104	0.143	0.286
0.500	-3.220	0.548	-1.004	12.1	0.064	0.005	0.108	0.147	0.288
0.550	-3.334	0.547	-0.959	12.0	0.055	-0.012	0.113	0.157	0.292
0.600	-3.439	0.546	-0.918	11.6	0.053	-0.028	0.113	0.167	0.296
0.650	-3.530	0.548	-0.895	11.3	0.050	-0.042	0.101	0.171	0.299
0.700	-3.606	0.552	-0.877	11.0	0.044	-0.054	0.084	0.169	0.302

0.750	-3.679	0.554	-0.852	10.8	0.034	-0.064	0.068	0.161	0.303
0.800	-3.756	0.555	-0.824	10.5	0.025	-0.072	0.056	0.153	0.304
0.850	-3.836	0.555	-0.792	10.2	0.017	-0.080	0.049	0.146	0.305
0.900	-3.916	0.554	-0.760	9.8	0.013	-0.086	0.047	0.143	0.304
0.950	-3.991	0.552	-0.729	9.5	0.010	-0.091	0.048	0.141	0.303
1.000	-4.058	0.550	-0.702	9.3	0.008	-0.095	0.050	0.140	0.301
1.100	-4.163	0.546	-0.662	9.0	0.004	-0.105	0.057	0.141	0.299
1.200	-4.230	0.541	-0.641	9.0	0.000	-0.116	0.060	0.143	0.298
1.300	-4.267	0.538	-0.636	9.2	-0.006	-0.132	0.060	0.144	0.298
1.400	-4.292	0.534	-0.637	9.4	-0.012	-0.153	0.056	0.142	0.298
1.500	-4.322	0.531	-0.637	9.6	-0.017	-0.175	0.052	0.142	0.298
1.600	-4.357	0.530	-0.638	9.7	-0.023	-0.196	0.049	0.142	0.298
1.700	-4.393	0.530	-0.641	9.7	-0.029	-0.215	0.046	0.143	0.300
1.800	-4.429	0.530	-0.646	9.8	-0.034	-0.232	0.043	0.144	0.302
1.900	-4.466	0.532	-0.653	9.8	-0.039	-0.252	0.040	0.145	0.305
2.000	-4.504	0.534	-0.662	9.8	-0.044	-0.278	0.037	0.147	0.308

Table A2. Derived scaling coefficients of the empirical GMPEs, for the region of former Yugoslavia—Equation 1, based on the regional PSA_{vert} data that were recorded at epicentral distances up to 30 km

T	a_1	a_2	a_3	r_0	a_4	a_5	a_6	a_7	σ
0.040	5.345	0.391	-5.302	40.0	0.156	0.041	-0.154	-0.008	0.266
0.042	5.346	0.391	-5.296	40.0	0.156	0.043	-0.153	-0.008	0.267
0.044	5.341	0.390	-5.287	40.0	0.155	0.045	-0.152	-0.008	0.267
0.046	5.330	0.390	-5.271	40.0	0.154	0.048	-0.152	-0.008	0.268
0.048	5.318	0.387	-5.246	40.0	0.147	0.050	-0.150	-0.008	0.269
0.050	5.308	0.385	-5.225	40.0	0.141	0.052	-0.149	-0.006	0.271
0.055	5.235	0.381	-5.146	40.0	0.129	0.057	-0.147	-0.007	0.273
0.060	5.109	0.380	-5.045	40.0	0.123	0.061	-0.147	-0.011	0.275
0.065	4.933	0.381	-4.920	40.0	0.122	0.066	-0.149	-0.018	0.276
0.070	4.738	0.385	-4.796	40.0	0.127	0.070	-0.153	-0.026	0.277
0.075	4.345	0.392	-4.564	40.0	0.143	0.074	-0.161	-0.044	0.277
0.080	3.972	0.397	-4.337	40.0	0.158	0.077	-0.173	-0.071	0.276
0.085	3.644	0.399	-4.127	40.0	0.169	0.081	-0.189	-0.104	0.275
0.090	3.412	0.399	-3.970	40.0	0.176	0.084	-0.207	-0.138	0.274
0.095	3.307	0.397	-3.889	40.0	0.180	0.087	-0.225	-0.169	0.272
0.100	3.366	0.396	-3.904	40.3	0.182	0.090	-0.241	-0.194	0.270
0.110	3.420	0.391	-3.908	40.1	0.182	0.095	-0.274	-0.229	0.267
0.120	2.819	0.388	-3.550	37.0	0.179	0.099	-0.306	-0.240	0.267
0.130	2.044	0.389	-3.112	33.4	0.175	0.102	-0.328	-0.230	0.268
0.140	1.471	0.396	-2.804	31.7	0.169	0.105	-0.335	-0.208	0.269
0.150	1.208	0.406	-2.687	31.5	0.162	0.107	-0.326	-0.178	0.270
0.160	1.287	0.417	-2.779	32.6	0.156	0.109	-0.302	-0.142	0.271
0.170	1.430	0.428	-2.914	33.9	0.150	0.110	-0.270	-0.103	0.273
0.180	1.684	0.438	-3.114	35.3	0.145	0.111	-0.233	-0.066	0.274
0.190	2.016	0.447	-3.357	36.7	0.139	0.111	-0.193	-0.031	0.274
0.200	2.371	0.454	-3.609	38.0	0.134	0.111	-0.153	0.001	0.273
0.220	2.928	0.464	-4.013	39.6	0.132	0.109	-0.076	0.056	0.271
0.240	3.132	0.468	-4.191	40.0	0.139	0.106	-0.008	0.099	0.268
0.260	3.229	0.471	-4.295	39.7	0.143	0.101	0.041	0.128	0.263
0.280	3.557	0.476	-4.531	39.9	0.133	0.095	0.068	0.146	0.259

0.300	3.945	0.484	-4.803	40.1	0.112	0.088	0.077	0.156	0.258
0.320	4.317	0.493	-5.067	40.2	0.087	0.081	0.074	0.163	0.258
0.340	4.640	0.506	-5.309	40.2	0.059	0.072	0.062	0.169	0.261
0.360	4.780	0.519	-5.446	40.0	0.034	0.064	0.050	0.173	0.264
0.380	4.825	0.531	-5.522	39.8	0.013	0.055	0.041	0.176	0.268
0.400	4.793	0.540	-5.545	39.6	-0.001	0.046	0.038	0.177	0.271
0.420	4.707	0.547	-5.530	39.6	-0.011	0.037	0.039	0.177	0.275
0.440	4.640	0.551	-5.517	39.6	-0.016	0.029	0.047	0.174	0.277
0.460	4.542	0.554	-5.484	39.5	-0.019	0.021	0.055	0.172	0.279
0.480	4.518	0.555	-5.489	39.6	-0.021	0.013	0.062	0.170	0.280
0.500	4.448	0.555	-5.463	39.6	-0.021	0.005	0.071	0.168	0.281
0.550	4.370	0.553	-5.446	39.8	-0.018	-0.012	0.083	0.168	0.283
0.600	4.287	0.552	-5.420	40.0	-0.014	-0.028	0.079	0.174	0.284
0.650	4.110	0.555	-5.344	40.1	-0.016	-0.042	0.059	0.181	0.286
0.700	3.922	0.559	-5.261	40.0	-0.024	-0.054	0.039	0.186	0.288
0.750	3.771	0.559	-5.189	40.0	-0.034	-0.064	0.027	0.188	0.289
0.800	3.627	0.558	-5.122	40.0	-0.045	-0.072	0.018	0.189	0.288
0.850	3.497	0.556	-5.062	40.0	-0.054	-0.080	0.014	0.190	0.287
0.900	3.369	0.554	-5.004	40.0	-0.059	-0.086	0.012	0.190	0.284
0.950	3.259	0.552	-4.955	40.0	-0.062	-0.091	0.012	0.190	0.282
1.000	3.163	0.549	-4.913	40.0	-0.063	-0.095	0.012	0.190	0.280
1.100	2.998	0.545	-4.845	40.0	-0.062	-0.105	0.012	0.188	0.275
1.200	2.872	0.543	-4.799	40.0	-0.058	-0.116	0.011	0.185	0.273
1.300	2.770	0.540	-4.765	40.0	-0.052	-0.132	0.009	0.182	0.272
1.400	2.657	0.536	-4.717	40.0	-0.048	-0.153	0.008	0.178	0.271
1.500	2.532	0.532	-4.661	40.0	-0.046	-0.175	0.007	0.175	0.270
1.600	2.423	0.529	-4.617	40.0	-0.044	-0.196	0.006	0.173	0.269
1.700	2.325	0.527	-4.581	40.0	-0.042	-0.215	0.006	0.171	0.268
1.800	2.237	0.526	-4.551	40.0	-0.041	-0.232	0.005	0.169	0.268
1.900	2.159	0.525	-4.529	40.0	-0.040	-0.252	0.005	0.168	0.268
2.000	2.092	0.526	-4.514	40.0	-0.040	-0.278	0.005	0.166	0.269